SIMULATION OF STARTING OF AN INDUCTION MOTOR DRIVEN BY A MODULAR MULTILEVEL CASCADE INVERTER WITHOUT SPEED SENSOR

MR. KISHOR PRATAP JADHAV
M. Tech, Fabtech Technical Campus College of Engineering and Research, Sangola, Solapur Maharashtra India.

MR. AKIREDDY SHRAVANKUMAR
Assistant Professor, Fabtech Technical Campus College of Engineering and Research, Sangola, Solapur Maharashtra India

ABSTRACT:

In this paper theoretical approach with proven mathematical model is described for a speed-sensor less startup method particularly for induction motor driven by a modular multilevel cascade inverter based on double-star chopper cells (MMCI-DSCC) from standstill to middle speed using PI controller. These types of motor are more suitable for large capacity fan – or blower type of load. While implementing this technique closed loop method is used as it is more robust and reliable as compared to open loop system. The simulation of above system is done in this paper and results are considerably good.

INDEX TERMS: Induction Motor Drives, Closed loop system, Modular multilevel converter (MMC), PI controller.

I. INTRODUCTION:

Attention has been paid to medium-voltage motor drives for energy saving without regenerative brakes [1]–[4]. A modular multilevel cascade inverter based on double star chopper cells (MMCI-DSCC) has been expected as one of the next-generation medium-voltage multilevel pulse width modulation (PWM) inverters for such motor drives [5]–[illegible]. For the sake of simplicity, the MMCI-DSCC is referred to as the "DSCC" in this paper [5]. Open loop control system can be converted to closed loop control system by providing a feedback. This feedback automatically makes the suitable changes in the output due to external disturbance. In this way closed loop control system is called automatic control system. A synergy effect of lower voltage steps and phase-shifted PWM leads to lower harmonic voltage and current, as well as lower EMI emission, as the count of cascaded chopper cells per leg increases. The power conversion circuit of the DSCC is so flexible in design that any count of cascaded chopper cells is theoretically possible [6].When a DSCC is applied to an ac motor drive, the DSCC would suffer from ac-voltage fluctuations in the dc-capacitor voltages of each chopper cell in a low-speed range, because the ac-voltage fluctuation gets more serious as a stator-current frequency gets lower [7]. Hence, the fluctuation should be attenuated satisfactorily to achieve stable low-speed and start-up performance. Several papers have exclusively discussed startup methods for DSCC-based induction motor drives [10]–[14].

The aim of this paper is to verify the effectiveness and practicability of a speed-Sensor less start-up method for a DSCC based induction motor drive, in which the motor starts rotating from standstill to middle speed with a ramp change. The start-up method discussed in this paper is characterized by combining capacitor voltage control with motor-speed control. The capacitor-voltage control plays a part in regulating the mean dc voltage of each of the dc capacitors [7] and in mitigating the ac voltage appearing across each dc capacitor, which fluctuates at the stator-current frequency [4]–[illegible].The motor-speed control relies on an equivalent circuit of an induction motor, which was proposed in [17]. The motor-speed control is based on "feedback" control of the stator current, which is the same as that in the slip-frequency control, whereas the commands for the amplitude and frequency of the stator current are based on "feed forward" control in consideration of a speed –versus - load- torque characteristic, as done in the V/f control.

II. CIRCUIT CONFIGURATION ANDCAPACITOR-VOLTAGE CONTROL OF THE DSCC:

A. CIRCUIT CONFIGURATION:

Fig. 1(a) shows the main circuit configuration of the DSCC discussed in this paper. Each leg consists of eight cascaded bidirectional chopper cells shown in Fig. 1(b) and a center tapped inductor per phase, as shown in Fig. 1(c). The center tap of each inductor is connected directly to each of the stator terminals of an induction motor, where it is the u-phase stator current. The center-tapped inductor is more cost effective than two no coupled inductors per leg, because the center tapped inductor presents inductance LZ only to the circulating current Z and no inductance to the stator current [7]. It brings significant reductions in size, weight, and cost of the magnetic core.1These advantages in the center-tapped inductor are mostly welcomed, particularly applications to motor drives, in which no ac inductors are required between the motor and the inverter. In Fig. 1, instantaneous current is Pu and iNu are the u phase positive- and negative-arm currents, respectively, and iZu is the u-phase circulating current defined as follows [7]:

$$i_{Zu} \triangleq \frac{1}{2}(i_{Pu} + i_{Nu}) \quad (1)$$

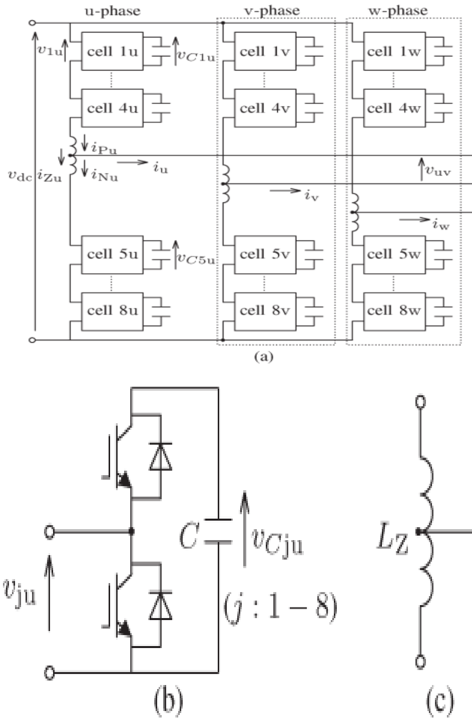

Fig.1. Circuit configuration for an MMCI-DSCC. (a) Power circuit. (b) Chopper cell. (c) Center-tapped inductor.

Note that iZu includes dc and ac components to be used for the capacitor-voltage control. The dc component flows from the common dc link to each leg, while the ac component circulates among [illegible]. The individual ac components included in the three-phase circulating currents ˜iZu,˜iZv, and [illegible] cancel each other out, so that no ac component appears in either motor current or dc-link current.

The arm currents iPu and iNu can be expressed as linear functions of two independent variables iu and iZu as follows [illegible]:

$$i_{Pu} = \frac{i_u}{2} + i_{Zu} \quad [illegible]$$

$$i_{Nu} = -\frac{i_u}{2} + i_{Zu} \quad (3)$$

The dc-capacitor voltage in each chopper cell consists of dc and ac components causing an ac-voltage fluctuation. No When neither common-mode voltage or ac circulating current is Superimposed, the peak-to-peak ac-voltage fluctuation ΔvCju is approximated as follows [10]:

$$\Delta_{vCju} \simeq \frac{\sqrt{2}I_1}{4\pi fc} \quad (4)$$

whereI1 is the rms value of the stator current, f is the frequency of the stator current, and Cis the capacitance value of each dc capacitor. According to (4),ΔvCju is inversely proportional to f and proportional toI1. Hence, ΔvCju increases as the stator-current frequency decreases.

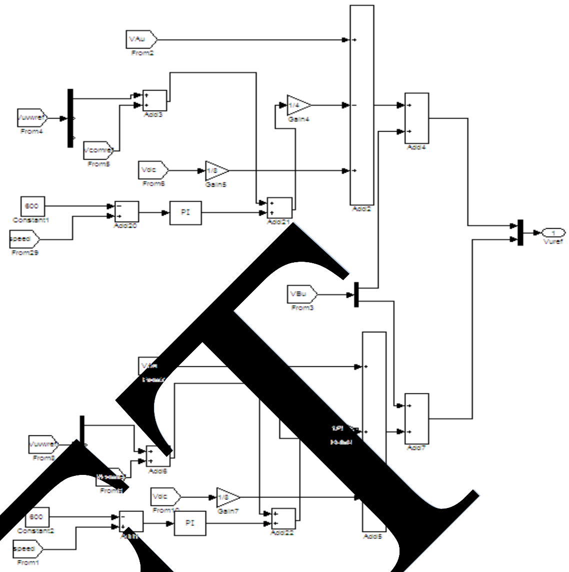

Fig. 2. Overall control block diagram

B. CAPACITOR-VOLTAGE CONTROL:

Fig. 2 shows the overall control block diagram of the startup method. The 24 dc-capacitor voltages *v* Cjuvw, the dc- link voltage *v*dc, and the six arm currents *i*Puvw and *i*Nuvw are detected, and they are input signals for the block diagram. Note that the three stator currents *i*uvw are calculated from the detected arm currents. This paper employs two kinds of existing capacitor-voltage control techniques for regulating the mean dc voltage of each dc capacitor and for mitigating the ac-voltage fluctuation at the stator-current frequency. The mean dc-voltage regulation can be achieved by using the "arm" balancing control applied to the six arms and the "individual" balancing control applied to the one arm at the same time [7]. The ac-voltage fluctuation can be mitigated by the sophisticated control discussed in [13]. This control interacts the common-mode voltage *v* com, which is injected to three center-tap terminals of the DSCC with the ac components of the three circulating currents ˜*i*Zuvw. This can mitigate the ac voltage fluctuation at the stator-current frequency, thus leading to start up from standstill. As a result, the remaining ac-voltage fluctuations are independent of the time-varying frequencies of the stator current, but dependent on a fixed frequency of the injected common-mode voltage (50 Hz in this experiment). The circulating- current feedback control included in the mean dc voltage regulation block yields a command voltage of *v a*∗.Fig. 3 shows the block diagram for the motor-speed control. The three-phase stator currents are transformed into dc quantities by using the d−q transformation to enhance current control ability.

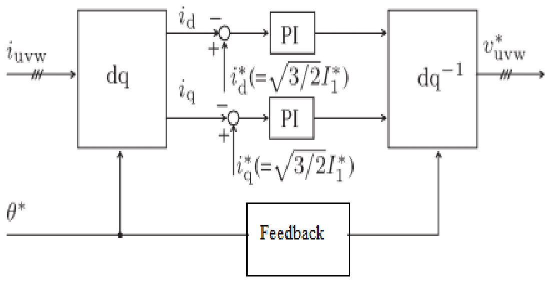

Fig.3. Block diagram of speed control with closed loop system

Finally, command u-phase voltages for each chopper cell,i.e.,v∗ju, are given as follows

$$v_{ju}^* = v_a^* + v_{Bju}^* - \frac{v_u^* + v_{com}^*}{4} + \frac{v_{dc}}{8} \; (j = 1-4) \quad (5)$$

$$v_{ju}^* = v_a^* + v_{Bju}^* + \frac{v_u^* + v_{com}^*}{4} + \frac{v_{dc}}{8} \; (j = 5-8) \quad (6)$$

Here, v∗a and v∗Bju are used to regulate the mean dc voltage, v∗u is the command motor voltage given by Fig. 3 described inthe later section,v∗comis the command common-mode voltage ,and vdc is the dc-link voltage used as feed forward control. The command rms value of the common-mode voltage V∗com should be set as high as possible to reduce the amplitude of each a circulating current, because it is inversely proportional to Vcom Moreover, there is no relationship between common-mode voltage and power rating of the motor.
In a low-speed range of f≤12Hz, the rms value of the common-mode voltage V∗com and the ac circulatingcurrents˜iZuvw are controlled actively to mitigate the a voltage fluctuation of each capacitor voltage [14].When f>20 Hz, neither V∗com nor ˜iZuvw is superimposed. During a frequency range of12≤f≤20Hz,V∗com, and ˜iZuvw decrease linearly in their amplitude. Note that the dc circulating current is used to regulate the mean dc voltage of each dc capacitor through all frequency range [10].

III. MOTOR-SPEED CONTROL:

This section describes a motor-speed control forming a feedback loop of three-phase stator currents for achieving a stable start-up of an induction motor. First, the motor-speed control is discussed in terms of a form and function. Second, it is compared with conventional motor-speed control techniques, i.e., "volts-per-hertz" and "slip-frequency" control techniques.

A. CONTROL PRINCIPLES:

The motor-speed control forms a feedback loop of threephase stator currents to realize a stable start-up from standstill. This requires the current sensors attached to the ac terminals. The stator current in one phase is calculated by the corresponding arm currents detected. Therefore, no additional currentsensor is required.

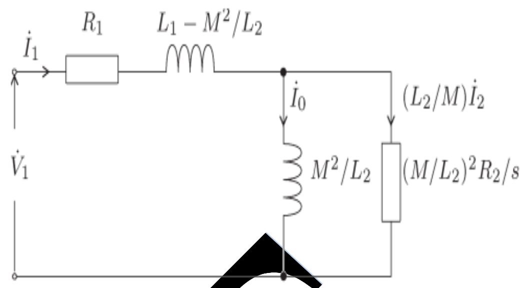

Fig. 4. Per-phase equivalent circuit based on the total linkage flux of the secondary windings

Fig.4 shows a per-phase equivalent circuit based on the total linkage flux of the secondary windings

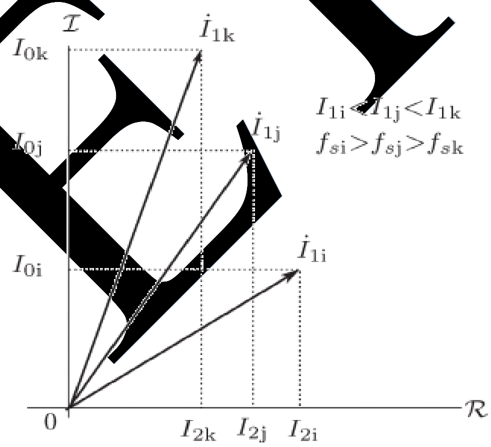

Fig.5. Phasor diagram for the stator currents with different amplitudes but the same torque

Quantities by using the d–q transformation to enhance current controllability. In Fig. 5.3,θ∗is the phase information used forth d–q transformation, whereas I ∗dand I∗qare the command currents given by

$$i_d^* = i_q^* = \sqrt{\frac{3}{2}} I_1^* \quad (7)$$

Where I∗1 is the command for the stator rms current. Note that I∗1 and f∗ are given not by feedback control, but by feed forward control, as described later.Fig.5.4 shows a per-phase equivalent circuit of an induction motor based on the total linkage flux of the secondary windings. Although this circuit is valid only under steady-state conditions, it is applicable to a fan- or blower-like load, in which the motor mechanical speed is adjusted slow enough to be considered as the steady-state condition. Here, ˙I1 is the phasor stator current, ˙I0 is the phasor magnetizing current, and ˙I2 is the phasor torque current. Note that˙I0 and˙I2 are orthogonal to each other in steady-state conditions. The rms value of˙I1, I1is given in as follows:

$$I_1=\sqrt{I_0^2+\left(\frac{L_2}{M}I_2\right)^2} \quad (8)$$

The motor torque TM is expressed by using I0 and I2 that are the rms values of˙I0and˙ I2, respectively, as follows :

$$T_M = 3PMI_0I_2 \quad (9)$$

Where P is the pole-pair number. Fig. 5 shows a phasor diagram for three different phasor stator currents ˙I1i,˙I1j, and˙I1kbut with producing the same torque ,in which a relation of I1i<I1j<I1k holds. The imaginary flame I corresponds to the magnetizing current I0, and the real flame R corresponds to the torque currentI2. It is obvious in (9) and Fig. 5 that the motor torque TM is proportional to the area of the triangle surrounded by ˙I1,I2, and I0.The motor-speed control has no capability to control the magnetizing current and the torque current independently. However, when the phasor stator current changes from ˙ I1ito˙I1j, the torque current decreases from I2i to I2j and the magnetizing current increases fromI0ito I0j, respectively, to keep the area of the triangle constant. In other words, both I0 and I2would change each of the amplitude automatically when ˙I1changes.The slip frequency fs is described by using I2 andI0 as follows:

$$F_s = \frac{R_2}{2\pi M}\frac{I_2}{I_0} \quad (10)$$

A relation of fsi>fsj>fsk exists in Fig.5.5, which are the slip frequencies at different operating points. The slip frequency has no freedom when f and I1 are given.

B. COMPARISONS OF THREE MOTOR-SPEED CONTROL TECHNIQUES:

Table I summarizes comparisons among the three motor speed control techniques with a focus on similarity and difference. The "volts-per-hertz" control or shortly "V/f" control has two independent variables V1 and f, in which V1 is the motor voltage and f is the stator frequency. On the other hand, the two dependent variables are the stator current I1 and the slip frequency fs. The V/f control is a straight forward speed control requiring no speed sensor, which is based on feed forward control of V1 andf. However, both motor and DSCC may suffer from an over current during the start-up or when a rapid change in torque occurs.The slip-frequency control has two independent variablesI1andfs, and the two dependent variables are V1 andf. Here, the commands for I1 and fs are determined by a feedback loop of the motor mechanical speed, thus requiring a speed sensor attached to the motor shaft. The slip-frequency control can provide a faster torque response than the V/f control because of the existence of a feedback control for the motor mechanical speed.

The motor-speed control proposed for the DSCC-based induction motor drive has two independent variablesI1 and f, and the two dependent variables areV1andfs. Unlike the slipfrequency control, the motor-speed control requires no speed sensor because the commands for I1 andf, i.e., I∗1 andf∗,are given not by feedback control, but by feed forward control,as done in the V/fcontrol. This implies that the motor speed control proposed in this paper is inferior to the slip frequency control, in terms of torque controllability. However, it is applicable to a fan- or blower-like load, where the load torque is changing relatively slow and predictable Moreover, no over current occurs during the start-up, or when a rapid change in torque occurs, because of the existence of a feedback control loop of the stator current.

An energy saving during a start-up does not make a significant contribution to total energy saving performance from a practical point of view because the motor power in a low speed range is negligible in applications such as fan- or blower-like loads. This means that a comparison of the three methods, in terms of energy saving performance during a start-up, does not make sense when fan- or blower-like loads are considered.

TABLE I
COMPARISONS AMONG EXISTING VOLTS-PER-HERTZ AND SLIP-FREQUENCY CONTROL TECHNIQUES AND THE PROPOSED MOTOR-SPEED CONTROL TECHNIQUE

	Volts-per-hertz control	Slip-frequency control	Proposed motor-speed control
Independent variables	V_1 and f	I_1 and f_s	I_1 and f
Dependent variables	I_1 and f_s	V_1 and f	V_1 and f_s
Voltage control	Feedforward	-	-
Current control	-	Feedback	Feedback
Speed sensor	No	Yes	No

Moreover, current stresses of the conventional motor-speed control techniques, the V/f and slip-frequency control, and the proposed motor-speed control technique are the same, at least, in a steady-state condition when a magnetizing current is set to the same value in all speed range.

IV. COMMAND STATOR CURRENTS:

This section describes how to determine the command of the stator rms currentI∗1 and the stator-current frequency f∗. Thef ollowing two methods can be used to determineI∗1andf∗:

• Determination from the equivalent circuit shown in Fig. 4 When a speed-versus-load-torque characteristic is known, the equivalent circuit shown in Fig. 4 can be used to determine I∗1 and f∗, along with the motor parameters including the moment of load inertia. The motor torque should satisfy the following equation during the start-up:

$$T_M - T_L > (J_M + J_L)\frac{d\omega_{rm}}{dt} \qquad (11)$$

Where TL is the load torque, JMis the moment of inertia of the motor, JLis that of the load, and ωrm is the mechanical angular velocity. The right-hand term on (11) corresponds to an acceleration torque for the start up.

For making analysis simple and easy, the following reasonable approximations are made.

• The stator-current frequency agrees well with its command f∗(i.e.,f=f∗).

• The slip frequency fs is much smaller than f (i.e., fsf).

• The moment of inertia of the loadJLis much larger thanthat of the motorJM(i.e.,JMJL).

These three assumptions are applicable to fan- or blower-like loads for the following reasons. The first assumption is valid because the motor frequency, or the motor mechanical speed, is adjusted slowly, e.g., spending a few or several minutes to complete its start-up procedure. The second assumption is reasonable for an induction motor. The third assumption is valid because JL is typically 50–100 times larger thanJM[illegible]. Finally, (11) is simplified as follows:

$$T_M - T_L > J_L \frac{2\pi}{P}\frac{df^*}{dt} \qquad (12)$$

Where ωrm =2πf∗/P. Equation (12) means that the acceleration torque is proportional to the [illegible] change in f∗. This suggests that the minimum torque required for the motor start-up is TM=TL, when the term on the right-hand side in (12) is small enough to be negligible. In other words, the [illegible] off ∗ should be set to be as small as possible to reduce the acceleration torque. The motor torque TM in Fig. 5 is proportional to the area surrounded by [illegible] I2, and I0. The stator rms current required to produce the motor torque gets the smallest when the following relation is met:

$$I_0 = \frac{[illegible]}{M} I_2 \quad (13)$$

$$I_2 = \sqrt{\frac{T_M}{3pL_2}} \qquad (14)$$

Finally,I1is obtained by substituting (14) into (8) as follows:

$$I_1 = \sqrt{\frac{2L_2T_M}{3PM2}} \quad (15)$$

TABLE II

CIRCUITPARAMETERSUSED IN THE SIMULATION

Rated active power		15 kW
Rated line-to-line rms voltage	V_S	400 V
Rated dc-link voltage	V_{dc}	570 V
Center-tapped inductor	L_Z	4.0 mH(12%)
DC capacitor of chopper cell	C	3.3 mF
DC-capacitor voltage	V_C	140 V
Unit capacitance constant	H	52 ms [19]
Cell count per leg	N	8
Triangular-wave-carrier frequency	f_C	2 kHz
Equivalent carrier frequency	Nf_C	16 kHz

DETERMINATION FROM SIMULATION:

When a speed-versus-[illegible]d-torque characteristic is unknown, the current command I∗1should be determine experimentally as follows. The initial value of I∗1is set to zero. Then, I∗1isbeing increased gradually where the motor starts rotating up. This method is similar to a traditional V/f control, in terms of no use of motor parameters. It is difficult to apply the motor-speed control to an application where a rapid or unpredictable change in [illegible] torque may happen. The reason is thatI∗1 and f∗ are given by feed forward control with no capability of handling a rapid or unpredictable change in torque. However, the motor-speed control is applicable to a fan- or blower-like load, where the motor mechanical speed is adjusted slow, and the load torque of which is proportional to a square of the motor mechanical spee In this case,I1should be given so that it is proportional to the command motor mechanical speed, as predicted from (15).

In addition,I1 is proportional to the stator-current frequency because the slip frequency sis typically negligible compared to the stator-current frequency(fsf). Finally, experimental adjustment of the slope ofI1/f(= I∗1/f∗)is required to achieve the stable start-up. The so-called "torque boost" function at low speeds, which is used in the V/f control, is applicable to the motor-speed control.

Closed loop system

The quantity of the output being measured is called the "feedback signal", and the type of control system which uses feedback signals to both control and adjusts itself is called a Close-loop System. A Closed-loop Control System, also known as a feedback control system is a control system which uses the concept of an open loop system as its forward path but has one or more feedback loops (hence its name) or paths between its output and its input. The reference to "feedback", simply means that some portion of the output is returned "back" to the input to form part of the systems excitation.

NOVATEUR PUBLICATIONS
International Journal Of Research Publications In Engineering And Technology [IJRPET]
ISSN: 2454-7875
VOLUME 3, ISSUE 2, Feb. -2017

CLOSED-LOOP SYSTEM TRANSFER FUNCTION:

The **Transfer Function** of any electrical or electronic control system is the mathematical relationship between the systems input and its output, and hence describes the behavior of the system. Note also that the ratio of the output of a particular device to its input represents its gain. Then we can correctly say that the output is always the transfer function of the system times the input. Consider the closed-loop system below.

TYPICAL CLOSED-LOOP SYSTEM REPRESENTATION:

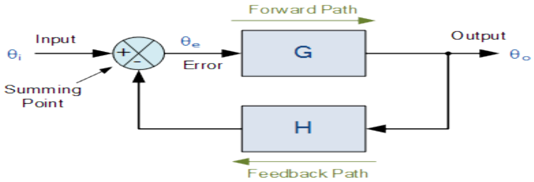

Fig 6.Bolck diagram of closed loop system

Where: block G represents the open-loop gains of the controller or system and is the forward path, and block H represents the gain of the sensor, transducer or measurement system in the feedback path.

To find the transfer function of the closed-loop system above, we must first calculate the output signal θo in terms of the input signal θi. To do so, we can easily write the equations of the given block-diagram as follows.

The output from the system is equal to: Output = G x Error

Note that the error signal, θe is also the input to the feed-forward block: G

The output from the summing point is equal to: Error = Input - H x Output

If H = 1 (unity feedback) then:

The output from the summing point will be: Error (θe) = Input - Output

Eliminating the error term, then:

The output is equal to: Output = G x (Input - H x Output)

Therefore: G x Input = Output + G x H x Output

Rearranging the above gives us the closed-loop transfer function of:

$$\frac{\text{output}}{\text{Input}} = \frac{\theta_0}{\theta_i} = \frac{G}{1+GH} \quad (16)$$

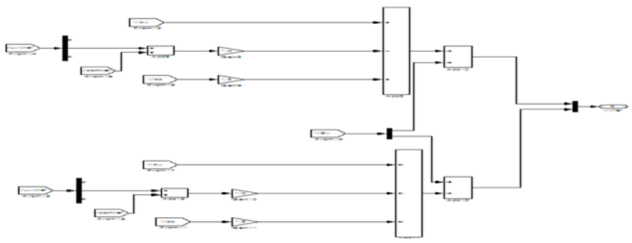

Fig.7 Closed loop block diagram of simulation

TABLE III
MOTOR PARAMETERS USED IN THE SIMULATION

Rated output power		15 kW
Rated frequency		50 Hz
Rated line-to-line rms voltage	V	380 V
Rated mechanical speed	N_{rm}	1460 min^{-1}
Rated stator rms current	I_1	32 A
Rated magnetizing current	I_0	18.4 A
Pole-pair number	P	2
Moment of motor inertia	J_M	0.1 kg · m^2
Moment of load inertia	J_L	0.1 kg · m^2

VI. SIMULATION RESULTS

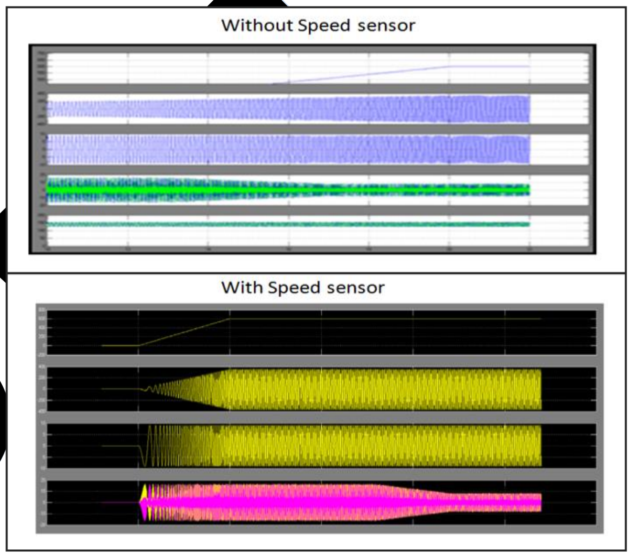

Fig.8. Simulation start-up waveforms when $I1*$ = 6.4 A (20%) and TL= 0%, where $I0$ = 6.4 A (35%).

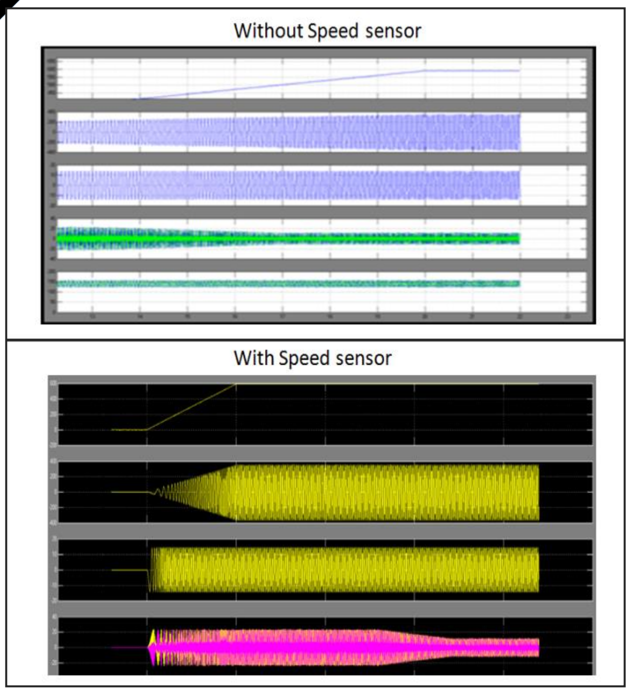

Fig.9 . Simulation start-up waveforms when I1∗ = 6.4 A (20%) and TL = 0%, where I0 = 6.4 A (35%).

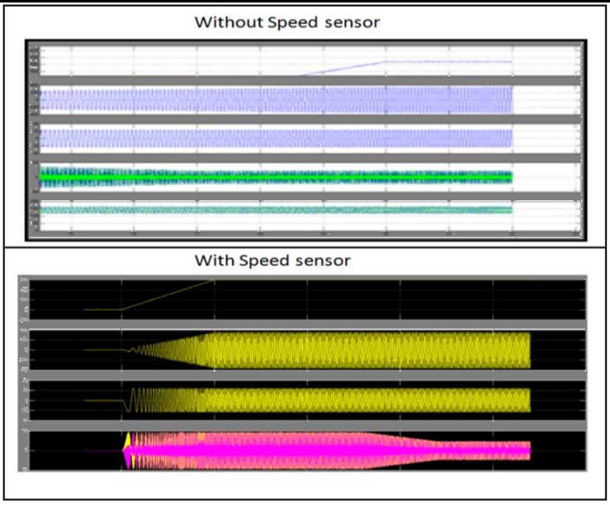

Fig.10. Simulation start-up waveforms when $I1*$ = 14 A (44%), and TL = 40%, where $I0$ = 9.9 A (54%).

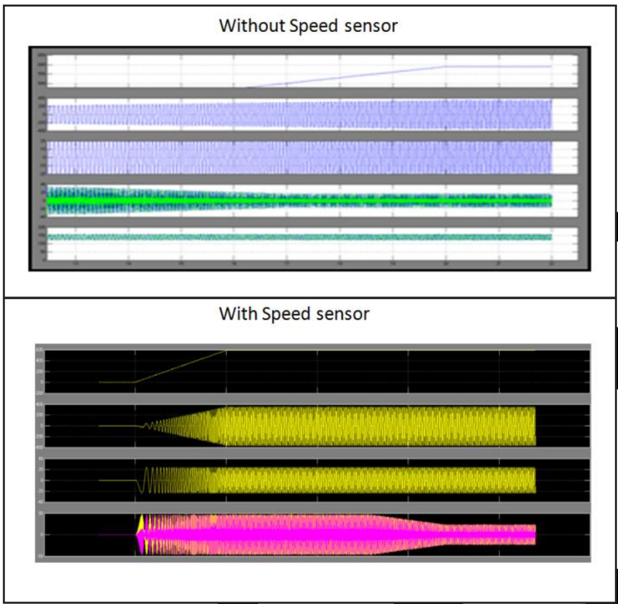

Fig.11. Simulation start-up waveforms when $I1*$ = 17 A (53%), and TL = 60%, where I0 = 12.0 A (65%).

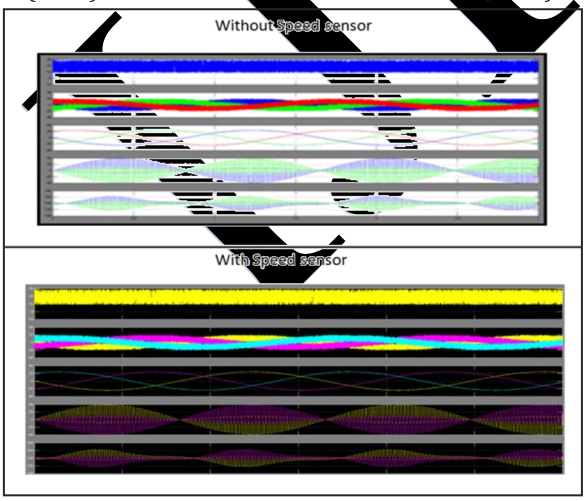

Fig.12. Simulation steady-state waveforms when $I1*$ = 17 A (5 3 %), $f*$ = 1 Hz, and TL = 60%, where I0 = 12.0 A (65%).

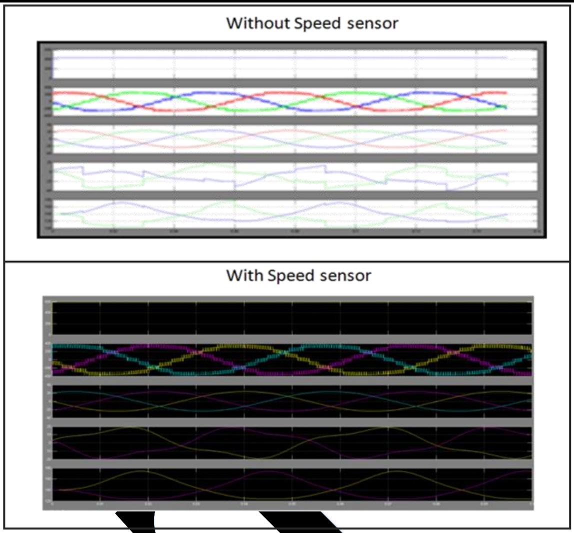

Fig. 13. Simulation steady-state waveforms when $I1*$ = 17 A (53%), $f*$ = 15 Hz, and TL = 60%, where I0 = 12.0 A (65%).

VII. CONCLUSION:

This paper has proposed a practical start-up method for DSCC-driven induction motor with no speed sensor from standstill to middle speed. This start-up method is characterized by combining capacitor-voltage control and motor-speed control.The motor-speed control with the optimal stator current under a load torque is based on the combination of feedback control of the three-phase stator currents with feedforward control of their amplitude and frequency. Feedback automatically makes the suitable changes in the output due to external disturbance. The arm-current amplitudes and ac-voltage fluctuations across each of the dc capacitors can be reduced to acceptable levels. Simulation results shown that the motor loaded with 60% can achieve a stable start up from standstill to a middle speed. The start-up torque has been increasing by a factor of three, without additional stress on both arm currents and ac-voltage fluctuations. This method is suitable particularly for adjustable-speed motor drives of large-capacity fans, blowers, and compressors for energy savings.

REFERENCES:

1) P. W. Hammond, "*A new approach to enhance power quality for medium voltage ac drives,*"IEEE Trans. Ind. Appl., vol. 33, no. 1, pp. 202–208, Jan./Feb. 1997.
2) R. Teodorescu, F. Blaabjerg, J. K. Pedersen, E.Cengelci, and P. N. Enjeti, "*Multilevel inverter by cascading industrial VSI,*"IEEE Trans. Ind. Appl.,vol. 49, no. 4, pp. 832–838, Jul./Aug. 2002.
3) J. Rodriguez, S. Bernet, J. O. Bin Wu, and S. Pontt, "*Multilevel voltage source-converter topologies for*

industrial medium-voltage drives," IEEE Trans. Ind. Electron, vol. 54, no. 6, pp. 2930–2945, Dec. 2007.

4) S. Malik and D. Kluge, "*ACS 1000 world's first standard ac drive for medium-voltage applications,"* ABB Rev., no. 2, pp. 4–11, 1998.
5) H. Akagi, "*Classification, terminology, and application of the modular multilevel cascade converter (MMCC),"*IEEE Trans. Power Electron.,vol. 26, no. 11, pp. 3119–3130, Nov. 2011.
6) A. Lesnicar and R. Marquardt, *"An innovative modular multilevel converter topology suitable for a wide power range,"* in Conf. Rec. IEEE Bologna Power Tech, 2003, [CD-ROM].
7) M. Hagiwara and H. Akagi, "*Control and experiment of pulse-width modulated modular multilevel converters,*" IEEE Trans. Power Electron., vol. 24, no. 7, pp. 1737–1746, Jul. 2009.
8) M. Hiller, D. Krug, R. Sommer, and S. Rohner, "*A new highly modular medium voltage converter topology for industrial drive applications,"* in Conf. Rec. EPE, 2009, pp. 1–10.
9) S. Rohner, J. Weber, and S. Bernet, "*Continuous model of modular multilevel converter with experimental verification,"* in Conf. Rec. IEEE-ECCE, 2011, pp. 4021–4028.
10) M. Hagiwara, K. Nishimura, and H. Akagi, "*A medium-voltage motor drive with a modular multilevel PWM inverter,"* IEEE Trans. Power Electron., vol. 25, no. 7, pp. [illegible], Jul. 2010.
11) A. Antonopoulos, L. Angquist, S. Norrga, K. Llves, and H. P. Nee, "*Modular multilevel converter ac motor drives with constant torque from zero to nominal speed,"* in Conf. Rec. IEEE-ECCE, 2012, pp. 739–746.
12) J. Kolb, F. Kammerer, and M. Braun, "*Dimensioning and design of a modular multilevel converter for drive applications,"* in Conf. Rec. EPE, 2012, pp. LS1a-1.1-1–LS1a-1.1-8, [CD-ROM].
13) A. J. Korn, M. Winkelnkemper, and P.Steimer, "*Low output frequency operation of the modular multilevel converter,"* in Conf. Rec. IEEE-ECCE, 2010, pp. 3993–3997.
14) M. Hagiwara, I. Hasegawa, and H. Akagi, "*Startup and low-speed operation of an adjustable-speed motor driven by a modular multilevel cascade inverter (MMCI),"* IEEE Trans. Ind. Appl., vol. 49, no. 4, pp. 1556–1565, Jul./Aug. 2013.
15) J. Holtz, "*Sensorless control of induction motor drives,*" Proc. IEEE, vol. 90, no. 8, pp. 1359–1394, Aug. 2002.
16) R. J. Pottebaum, "*Optimal characteristics of a variable-frequency centrifugal pump motor drive,* "IEEE Trans. Ind. Appl., vol. 20, no. 1, pp. 23–31, Jan. 1984.
17) N. Hirotami, H. Akagi, I. Takahashi, and A. Nabae, *"A new equivalent circuit of induction motor based on the total linkage flux of the secondary windings,"* Elect. Eng. Japan, vol. 103, no. 2, pp. 68–73, Mar./Apr. 1983.
18) A. Munoz-Garcia, T. A. Lipo, and D. W. Novotny, "*A new induction motor V/f control method capable of high-performance regulation at low speeds,"* IEEE Trans. Ind. Appl., vol. 34, no. 4, pp. 813–821, Jul./Aug. 1998.
19) [19] H. Fujita, S. Tominaga, and H. Akagi, "Analysis and design of a dc voltage-controlled static var compensator using quad-series voltage source inverters ,"IEEE Trans. Ind. Appl., vol. 32, no. 4, pp. 970–977,Jul./Aug. 1996.
20) H. Peng, M. Hagiwara, and H. Akagi, "*Modeling and analysis of switching-ripple voltage on the dc link between a diode rectifier and a modular multilevel cascade inverter (MMCI),"* IEEE Trans. Power. Electron., vol. 28, no. 1, pp. 75–84, Jan. 2013.

MR. KISHOR RPRATAP JADHAV

Completed B.E in Electrical &Electronics Engineering in 2014 from SRTM University, Nanded, Maharashtra and Pursuing M.E from Fabtech Technical Campus College of Engineering and Research, Sangola,solapur Maharashtra India.

E-mail id:**kishor.jadhav92921@gmail.com**

Mr. Akireddy Shravankumar

B.Tech. (Electrical & Electronics Engineering) from Kamala Institute of Technology & Science, JNTU Hyderabad in 2006 and M.Tech.(Electrical Power Systems) from Walchand College of Engineering, Sangli in 2009.Working as Assistant Professor in Electrical Engineering Department at Fabtech Technical Campus College of Engineering and Research, Sangola, solapur Maharashtra India.

E-mail id: **shravan249@gmail.com**